Preprints, 4th IFAC Conference on
Advances in Proportional-Integral-Derivative Control
Almería, Spain | June 12-14, 2024

Design of PD Controllers with Input Saturation for Postprandial Blood Glucose Regulation ⋆

Ricardo Sanz * **Iván Sala-Mira** * **Pedro García** *,** **José-Luis Díez** *,** **Jorge Bondia** *,**

* *Instituto Universitario de Automática e Informática Industrial, Universitat Politècnica de València, Camino de Vera, s/n, 46022, Valencia, Spain (e-mail: risanda@upv.es; ivsami@upv.es)*
** *Centro de Investigación Biomédica en Red de Diabetes y Enfermedades Metabólicas Asociadas, Instituto de Salud Carlos III, Av. Monforte de Lemos 3-5, Madrid, Spain (e-mail: pggil@isa.upv.es; jldiez@isa.upv.es; jbondia@isa.upv.es).*

Abstract: An artificial pancreas system regulates blood glucose in people with type 1 diabetes by automating the appropriate insulin infusion rate calculation. Insulin cannot be removed once injected, and thus, the control input is constrained to be positive. Controllers designed without taking this constraint into consideration often deliver an excessive insulin dose after a meal intake (postprandial period), which may cause hypoglycemia, a condition related to harmful complications. The non-negativeness is usually handled indirectly through additional control structures that compensate for the saturation by cutting off the insulin flow in advance. The few approaches that consider the non-negativeness of insulin in the controller design process end up with high-order controllers, which are difficult to analyze. In this work, the design of a input-constrained PD controller for regulating postprandial glucose is explored. The set of feasible controller parameters is computed and related to the meal and insulin dynamics.

Keywords: type 1 diabetes, artificial pancreas, postprandial control, PID controllers, positive control

1. INTRODUCTION

Type 1 diabetes is a chronic disease where the pancreas no longer produces insulin. Cells need insulin to uptake glucose for fueling purposes (Alsahli et al., 2017). As a result, people with type 1 diabetes need exogenous insulin administration to survive. The application of control engineering to the glucose regulation problem has led to the artificial pancreas system (Nwokolo and Hovorka, 2023): a control system that automatically computes the insulin infusion to be administrated with an insulin pump upon glucose readings obtained with a continuous glucose monitoring device.

The glucose-insulin regulatory dynamic process constitutes an example of a system with positive input constraint: the insulin infusion must be non-negative since it cannot be extracted from the body once infused, disappearance being subjected to natural insulin degradation once fully absorbed from the subcutaneous tissue. This feature limits the glucose control performance, which is specially revealed when compensating for meal intakes (postprandial control). The meal carbohydrate content usually increases blood glucose levels at a fast rate compared to the slow effect of insulin, limited by the long delays during its subcutaneous absorption (Gingras et al., 2018). Aggressive controllers may be designed in an attempt to compensate for the slow process dynamics. However, doing so without considering the control input saturation will lead to insulin overdose, causing abnormally low glucose levels (hypoglycemia), a condition related to short-term adverse effects if it is not treated timely, such as seizure, cardiac arrest, coma, or death (Faradji et al., 2019).

Due to the non-negativeness nature of the control action, the ideal method to compensate for a meal with a low risk of hypoglycemia is to deliver an insulin bolus, i.e., an impulse-like feedforward action, prior to mealtime (Goodwin et al., 2015). This strategy has been successfully adopted for commercial artificial pancreas systems, outperforming conventional open-loop therapies (Boughton et al., 2019; Bassi et al., 2023). However, to calculate an insulin bolus, users must inform the controller about the carbohydrate content of their meals, a complex and burdensome task that should be removed in the next generation of artificial pancreas systems.

To handle unannounced meals, most of the controllers in the literature, except those based on receding horizon strategies, do not consider the control input constraint during the design process. Instead, they include addi-

⋆ This work was partially supported by grant PID2019-107722RB-C21 funded by MCIN/AEI/10.13039/501100011033, CIPROM/2021/012 funded by Conselleria de Innovación, Universidades, Ciencia y Sociedad Digital from Generalitat Valenciana. Corresponding author: Jorge Bondia (jbondia@isa.upv.es).

tional modules that inhibit insulin infusion to avoid hypoglycemia (Dovc et al., 2020; Cai et al., 2020; Sanz et al., 2021; Sala-Mira et al., 2022). In contrast, (Sereno et al., 2018), (Homayounzade, 2022), and (Sanz et al., 2023) are a few examples that directly treat the non-negativity of the insulin during the controller design process. However, these methodologies lead to high-order controllers or require elaborate state observers.

In this work, the design of low-order positive controllers for postprandial control is addressed. Specifically, a PD controller is designed based on the conditions detailed in (Lin and Fang, 1997) that characterizes non-overshooting and monotone nondecreasing steps response of a third-order linear system. This low-order controller allows to study how the insulin and meal dynamics affect the regions of feasible controller parameters.

1.1 Problem statement

The postprandial glucose regulation problem is cast into the feedback control loop depicted in Fig. 1. The plant and disturbance processes are assumed to be given by

$$G_d(s) = \frac{k_d}{(\tau_0 s + 1)(\tau_d s + 1)} \tag{1}$$

and

$$G_u(s) = \frac{-k_u}{(\tau_0 s + 1)(\tau_u s + 1)} \tag{2}$$

respectively, in which all constants are positive. In the diabetes context, the structure of these transfer functions correpond to simplifications of standard models in the literature (Heusden et al., 2012; Colmegna et al., 2014; Gondhalekar et al., 2016; Sanz et al., 2023), where G_u represents the effect of insulin in lowering blood glucose levels whereas G_d represents the glucose rise that occurs after a meal intake, modeled by an impulse disturbance $d(s)$. These linear models are obtained at an equilibrium point, the so-called basal glucose level y_b, that is achieved by a basal insulin infusion rate u_b. The control input u and the controlled output y are then incremental with respect to u_b and y_b, respectively. At this point, it should be remarked that the actual constraint on the control input is $u(t) \geq -u_b$, which implies zero insulin flow. However, the subsequent analysis is performed assuming that $u(t)$ must be positive. The conservatism of this assumption will be addressed in Section 4.

Note that both transfer functions have a common pole at $s = -1/\tau_0$, which is related to the glucose self-regulation dynamics at the equilibrium point. The distinct poles $-1/\tau_u$ and $-1/\tau_d$ represent the insulin and meal absorption dynamics, respectively. Typically, one has that $\tau_d \ll \tau_u$, that is, the meal effect is much faster than the insulin dynamics (Gingras et al., 2018). It has been shown in the literature that high-order feedback controllers approaching optimal performance can be constructed (Sanz et al., 2023), which guarantee the positiveness of the control signal after a meal intake. In this paper, the design of low-order controllers that guarantee this constraint is investigated. More specifically, proportional-derivative controllers of the form

$$C(s) = -(\alpha + \beta \cdot s) \tag{3}$$

are considered, with positive gains $\alpha, \beta \geq 0$. Note that the negative sign in (3) is included, without loss of generality,

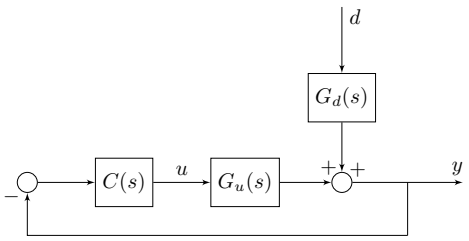

Fig. 1. Feedback control loop.

so that the controller gains are positive. The closed-loop relationship from d to u in the feedback control loop depicted in Fig. 1 is given by

$$G_{du}(s) \triangleq \frac{u(s)}{d(s)} = \frac{-C(s)G_d(s)}{1 + C(s)G_u(s)} \tag{4}$$

The control signal after a meal intake is given by the impulse response of (4). In what follows, the combinations of (α, β) that lead to a positive control input after a meal intake, that is, $\mathcal{L}^{-1}\{G_{du}(s)\}(t) \geq 0, \forall t$, will be determined.

2. CONTROLLER DESIGN

Using (3) into (4), the control input after a meal intake is given by

$$G_{du}(s) = \frac{k_d k_u^{-1}(\tau_u s + 1)(\bar{\alpha} + \bar{\beta} s)}{(\tau_d s + 1)(\tau_0 \tau_u s^2 + (\tau_0 + \tau_u + \bar{\beta})s + 1 + \bar{\alpha})} \tag{5}$$

where

$$\bar{\alpha} \triangleq k_u \alpha \geq 0 \qquad \text{and} \qquad \bar{\beta} \triangleq k_u \beta \geq 0 \tag{6}$$

have been defined for convenience. The poles of (5), denoted by r_1, r_2, r_3, are computed as

$$\begin{aligned} r_1 &= \frac{-(\tau_0 + \tau_u + \bar{\beta}) + \sqrt{\Delta}}{2\tau_0 \tau_u} \\ r_2 &= \frac{-(\tau_0 + \tau_u + \bar{\beta}) - \sqrt{\Delta}}{2\tau_0 \tau_u} \\ r_3 &= -1/\tau_d \end{aligned} \tag{7}$$

where Δ is the discriminant of the corresponding second-order polynomial equation, given by

$$\Delta = (\tau_0 + \tau_u + \bar{\beta})^2 - 4\tau_0 \tau_u (1 + \bar{\alpha}). \tag{8}$$

For simplicity, the subsequent analysis is limited to the case in which (5) has distinct real poles, that is, when $\Delta > 0$ holds (Lin and Fang, 1997). Using (8), this condition is fulfilled if

$$\bar{\alpha} < \frac{(\tau_0 + \tau_u + \bar{\beta})^2}{4\tau_0 \tau_u} - 1, \tag{9}$$

which leads to distinct real closed-loop poles. Furthermore, provided that $\Delta > 0$ holds, the closed-loop stability condition is easily obtained from (7) as $\bar{\alpha} > -1$. Therefore, it is clear that (6) and (9) guarantee that $r_1, r_2, r_3 < 0$ are distinct real stable closed-loop poles.

In order to apply the conditions reported in (Lin and Fang, 1997), the transfer function (5) is expressed in the following form

$$G_{du}(s) \triangleq K \frac{cs^3 + bs^2 + as + 1}{(t_1 s + 1)(t_2 s + 1)(t_3 s + 1)} \tag{10}$$

with $K = k_d k_u^{-1} \bar{\alpha}(1 + \bar{\alpha})^{-1}$,

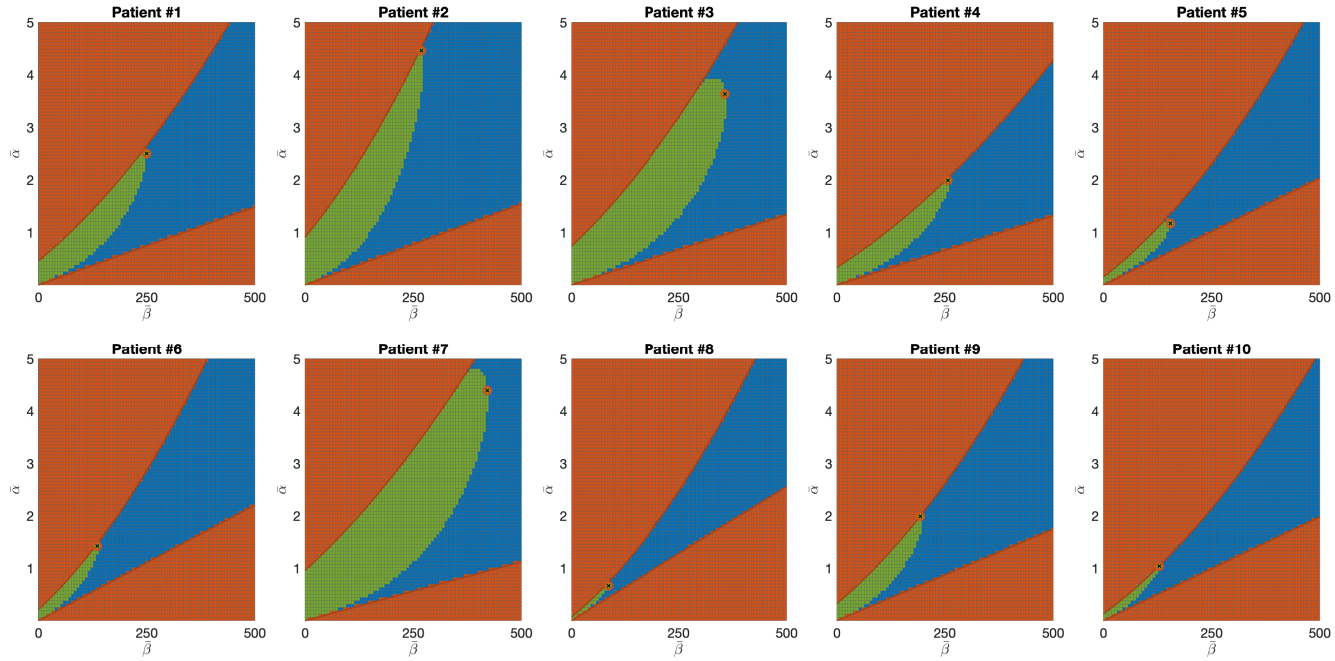

Fig. 2. Representation of the $(\bar{\alpha}, \bar{\beta})$-regions for the 10 virtual subjects. Feasible regions fulfilling the conditions (13)-(14) are represented in green. Circles denote the combination of α and $\bar{\beta}$ within the feasible region that achieve the lowest postprandial peak (best tuning). Regions leading to real and complex poles are shown in blue and red, respectively.

$$c = 0, \qquad b = \tau_u \frac{\bar{\beta}}{\bar{\alpha}}, \qquad a = \tau_u + \frac{\bar{\beta}}{\bar{\alpha}} \tag{11}$$

$$\begin{aligned} t_3 &= \min\left\{\tau_d, \frac{2\tau_0\tau_u}{\tau_0 + \tau_u + \bar{\beta} + \sqrt{\Delta}}\right\} \\ t_2 &= \max\left\{\tau_d, \frac{2\tau_0\tau_u}{\tau_0 + \tau_u + \bar{\beta} + \sqrt{\Delta}}\right\} \\ t_1 &= \frac{2\tau_0\tau_u}{\tau_0 + \tau_u + \bar{\beta} - \sqrt{\Delta}} \end{aligned} \tag{12}$$

where the latter are selected such that $t_1 > t_2 > t_3 > 0$. According to (Lin and Fang, 1997), the transfer function (5) has a positive impulse response if one of the following conditions holds

$$\begin{aligned} &\mathcal{R}_1 = (\mathcal{C}_1 \leq 0) \wedge (\mathcal{C}_2 \geq 0) \\ &\mathcal{R}_2 = (\mathcal{C}_2 < 0) \wedge (\mathcal{C}_4 \geq 0) \\ &\mathcal{R}_3 = (\mathcal{C}_1 \leq 0) \wedge (\mathcal{C}_2 < 0) \wedge (\mathcal{C}_4 < 0) \wedge (\mathcal{C}_5 \geq 0) \end{aligned} \tag{13}$$

where

Table 1. Identified parameters

Subject ID	k_u $\frac{\text{mg/dL}}{\text{pmol/kg/min}}$	k_d $\frac{\text{mg/dL}}{\text{g/mg/min}}$	τ_0 min	τ_u min	τ_d min
1	-191.5	6.19×10^4	336	94	23.9
2	-182.7	4.92×10^4	324	59	13.8
3	-124.6	6.02×10^4	373	78	34.2
4	-184.7	5.80×10^4	379	126	31.5
5	-121.8	6.00×10^4	246	115	57.0
6	-66.8	4.77×10^4	226	92	25.0
7	-207.7	7.81×10^4	445	79	29.2
8	-93.8	7.10×10^4	195	116	52.4
9	-169.1	5.33×10^4	286	97	27.1
10	-86.3	3.77×10^4	252	124	28.1

$$\begin{aligned} \mathcal{C}_1 &= t_1^2(a - t_1) - t_1 b \\ \mathcal{C}_2 &= t_2^2(a - t_2) - t_2 b \\ \mathcal{C}_3 &= t_3^2(a - t_3) - t_3 b \\ \mathcal{C}_4 &= t_2 t_3 a - (t_2 + t_3) b \\ \mathcal{C}_5 &= \frac{t_1(t_2 - t_3)}{t_3(t_1 - t_2)} \ln \frac{t_2^3 \mathcal{C}_1}{t_1^3 \mathcal{C}_2} - \ln \frac{t_3^3 \mathcal{C}_2}{t_2^3 \mathcal{C}_3} \end{aligned} \tag{14}$$

The conditions (13)-(14) reduce the feasible $(\bar{\alpha}, \bar{\beta})$ to a subset of the parameter space, denoted by $\mathcal{R} = \{(\bar{\alpha}, \bar{\beta}) : \mathcal{R}_1 \vee \mathcal{R}_2 \vee \mathcal{R}_3\}$. Within that subset, the proposed tuning is based on minimizing the peak of the postprandial response, given by $y(t) = \mathcal{L}^{-1}\{G_{dy}(s)d(s)\}(t)$, where

$$G_{dy}(s) \triangleq \frac{y(s)}{d(s)} = \frac{-G_d(s)}{1 + C(s)G_u(s)} \tag{15}$$

Since $d(s)$ is an impulse disturbance, the proposed design can be stated as

$$(\bar{\alpha}^*, \bar{\beta}^*) = \underset{(\bar{\alpha},\bar{\beta})\in\mathcal{R}}{\arg\min} \left\|\mathcal{L}^{-1}\left\{G_{dy}(s)\right\}(t)\right\|_\infty \tag{16}$$

3. CASE STUDY

To study the feasibility of the methodology described in the above section, the conditions (13)-(14) were applied to the 10 virtual subjects identified from the adult cohort of the UVa/Padova simulator (Dalla Man et al., 2014). This simulator is widely used in the field since it is the only one that received approval from the Food and Drug Administration for being a substitute for preclinical trials with animals. The identification scenario consisted of two announced meals, one with an overestimated insulin

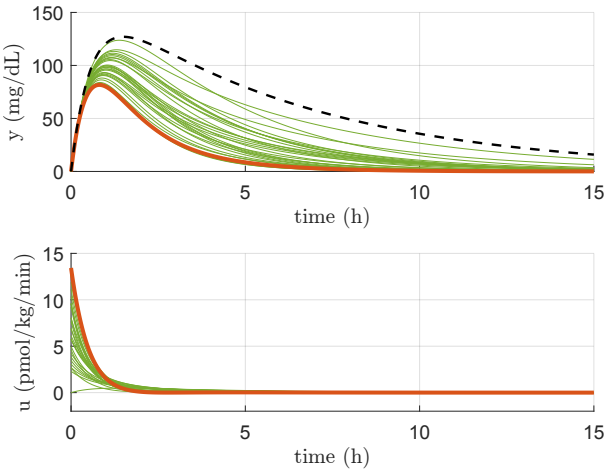

Fig. 3. Unit impulse disturbance responses for subject #3: incremental glucose (top) and incremental insulin (bottom). Green lines correspond to the responses with a sample of $(\bar{\alpha}, \bar{\beta})$ taken from the feasible region. The red line represents the best tuning inside the feasible region. The dashed black line shows the open-loop response of $G_d(s)$.

bolus and another with an underestimated bolus. The parameters of the transfer functions (1)–(2) were obtained by minimizing the root-mean-squared output error. The identified parameters are shown in Table 1. The following subsections study the feasibility of the positive regions in more detail.

3.1 Feasible $(\bar{\alpha}, \bar{\beta})$-regions

The conditions (13)-(14) were computed for each patient by partitioning the $(\bar{\alpha}, \bar{\beta})$-space, leading to the feasibility regions shown in Fig. 2. The red regions correspond to the $(\bar{\alpha}, \bar{\beta})$ combinations that lead to complex poles, which are not considered for simplicity, as stated in the previous section. The combinations of parameters that fulfill (13)-(14) are highlighted in green, which are embedded into the blue region, corresponding to real poles, that is, $\Delta > 0$. The parameters corresponding to the solution of the minimization problem (16) are marked with circles.

The results of the proposed tuning methodology are illustrated next. The patient #3, which has a large feasible region, was chosen as an example. The ideal closed-loop responses, given by (4), for all the controller parameters in the partitioned space, were computed under a unit impulse disturbance, corresponding to a meal size with a carbohydrate content of 1 g/BW, where BW refers to the patient body weight. The ideal closed-loop trajectories are shown in Fig. 3 (green). One can see that all control input signals satisfy $u(t) > 0$ for all t. Moreover, the response corresponding to $(\bar{\alpha}^*, \bar{\beta}^*)$ is highlighted in red, which indeed yields the best performance (minimum peak). For illustration purposes, the open-loop response of G_d is also shown (dashed-black), representing the effect the meal would have with no incremental insulin delivery. It should be pointed out that the proposed tuning considerably reduces the postprandial peak without increasing hypoglycemia.

3.2 Influence of plant dynamics on the $(\bar{\alpha}, \bar{\beta})$-regions

Meals and insulin may have different dynamics even for the same patient due to the variability in the meal or insulin absorption, the different nutritional composition of meals, and the different formulations of insulin. For this reason, it may be interesting to assess how the model paramters impact the size of the feasible regions.

To this end, first of all a way to measure the size of feasible regions is needed. A normalized size $S_{\mathcal{R}} \in [0, 1]$ is computed by dividing the area of the feasible region and the maximum area that region could have within the considered space partition. Then, for each patient three sensitivity analysis were carried out by varying one of the parameters $\{\tau_d, \tau_u, \tau_0\}$ one at a time while keeping the others constant. The parameters were varied within the intervals $\tau_d \in [0, \tau_u]$, $\tau_u \in [\tau_d, \tau_0]$ and $\tau_0 \in [0, \infty)$. Note that these intervals are different for each patient. Therefore, in order normalize the results among patients, the sensitivity analysis is reported in terms of the new parameters

$$\theta_d(x) = \frac{x}{\tau_u}, \quad \theta_u(x) = \frac{x - \tau_d}{\tau_0 - \tau_d}, \quad \theta_0(x) = 1 - \frac{\tau_u}{x}, \quad (17)$$

which perform the mappings $\theta_d(\tau_d) : [0, \tau_u] \to [0, 1]$, $\theta_u(\tau_u) : [\tau_d, \tau_0] \to [0, 1]$ and $\theta_0(\tau_0) : [0, \infty) \to [0, 1)$.

The results are shown in Figure 4. As the figure shows, for all patients, the feasible region expands for increasing values of θ_d (or τ_d) and decreasing values of θ_u (or τ_u). In other words, slower meals and faster insulin analogs increase the achievable performance. On the other hand, increasing the parameter θ_0 (or τ_0) also results in a monotone increment of the feasible region size. Finally, one limit behavior should be pointed out. Note that the feasible regions become arbitrarily large when $\theta_0 \to 1$. The same occurs when $\theta_d \to 1$ or $\theta_u \to 0$, which in turn imply $\tau_d \to \tau_u$, which is in accordance, for instance, with improved postprandial control in dual-hormone systems with insulin and pramlintide, where pramlintide slows

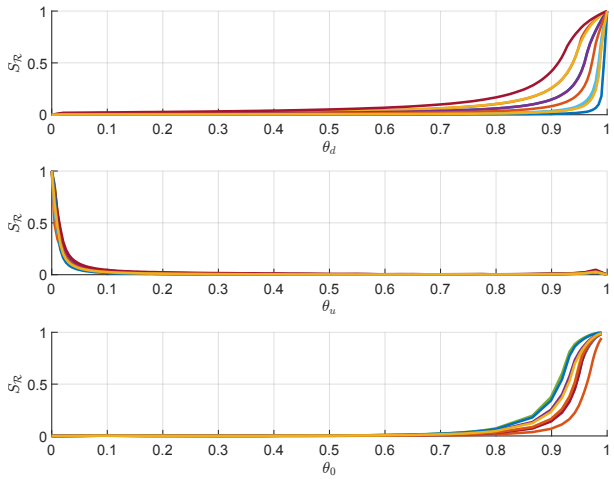

Fig. 4. Influence of insulin and meal dynamics onto the feasible region size for the 10 virtual subjects. $S_{\mathcal{R}}$ denotes the normalized size of the feasible regions. θ_d, θ_u, and θ_0 are the normalized values of τ_d, τ_u, and τ_0.

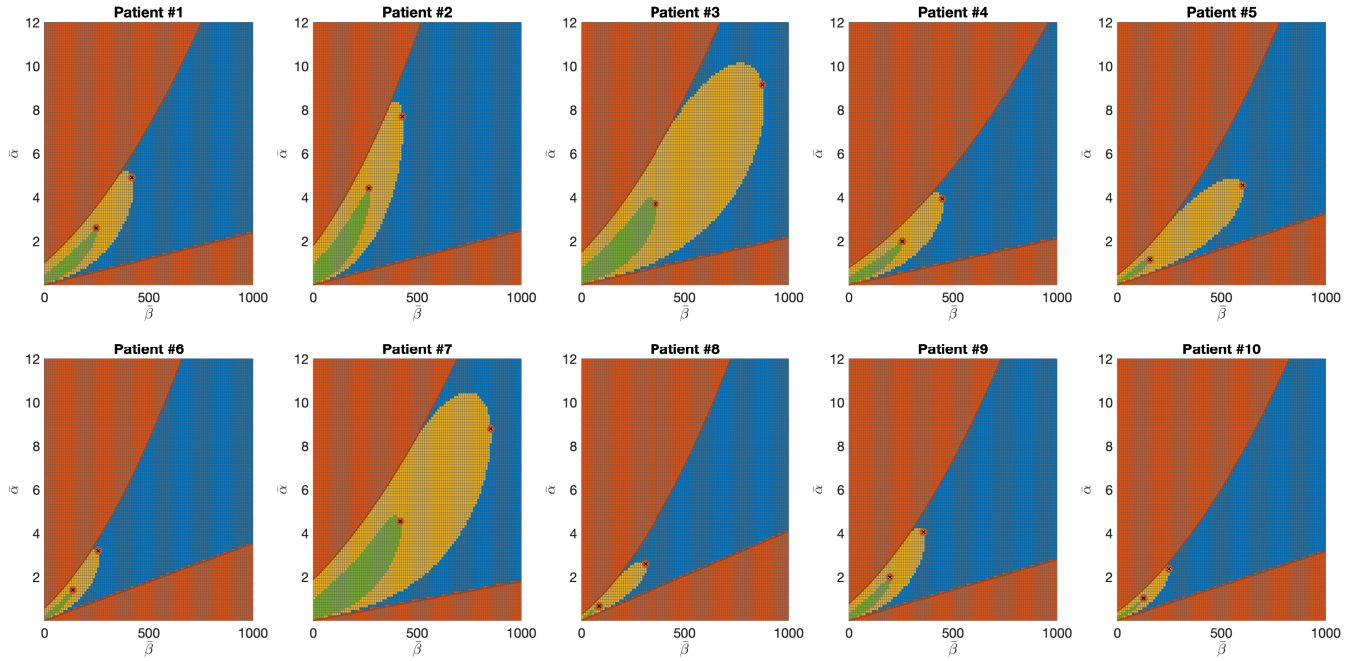

Fig. 5. Representation of the extended $(\bar{\alpha}, \bar{\beta})$-regions for the 10 virtual subjects. Red regions represents the combinations fulfilling (13)-(14) with a 25% variation in the time constants, while green regions correspond to the actual feasible regions shown in Fig. 2. Circles denote the combination of α and $\bar{\beta}$ within the feasible region that achieve the lowest postprandial peak (best tuning).

down meal dynamics, i.e., τ_d, by delaying gastric emptying (Haidar et al., 2020).

4. REDUCING THE CONSERVATISM OF THE CONTROLLER

The whole analysis performed so far has relied on the assumption that only positive control actions are feasible. As discussed in the Introduction, this is a conservative assumption. In the previous subsection, the influence of the open-loop plant parameters on the size of the feasibility region was established. Therefore, a naive approach to reduce conservatism is to perform the analysis upon slightly modified parameters τ_0, τ_d and τ_u so as to enlarge the resulting region and thus violate the positivity constraint by a small amount.

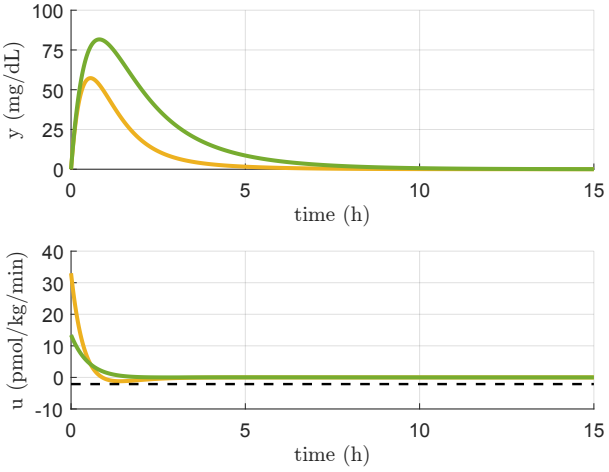

Fig. 6. Comparison of the unit impulse disturbance response for the original feasible region (green) and the extended region (yellow). The dashed line in the bottom panel indicates the $-u_b$ threshold.

In order to illustrate this approach, the analysis in Section 3.1 was repeated increasing τ_0, τ_d by 25% and reducing τ_u by the same amount. The resulting regions are depicted in Fig. 5 (yellow) along with the original ones (green). One can see that the regions are significantly enlarged with respect to the originals. The best-performance tuning in both cases is marked with circles. The new tuning is illustrated again using Patient #3. The results are shown in Fig. 6. The response with the new tuning (red) leads to a smaller postprandial peak (green). Furthermore, the new control signal (yellow) does not fulfill the positivity constraint by a small amount, as expected, without reaching the minimum value $-u_b$ (dashed-black). Note that this result was obtained by trial-and-error changing the percentage of variation in the aforementioned parameters.

5. CONCLUSION

In this article, a PD controller that ensures a non-negative control action is designed for the postprandial control of patients with type 1 diabetes. Simulations show that the proposed controller reduces the postprandial peak while keeping the insulin positive. In addition, the impact of the meal and insulin dynamics on the feasibility of the controller has been studied. This analysis showed that the difference between the insulin and meal dynamics

considerably influences the size of the feasible regions and thus plays a crucial role in the achievable performance.

REFERENCES

Alsahli, M., Shrayyef, M.Z., and Gerich, J.E. (2017). *Normal Glucose Homeostasis*, 23–42. Springer International Publishing.

Bassi, M., Franzone, D., Dufour, F., Strati, M.F., Scalas, M., Tantari, G., Aloi, C., Salina, A., d'Annunzio, G., Maghnie, M., and Minuto, N. (2023). Automated insulin delivery (aid) systems: Use and efficacy in children and adults with type 1 diabetes and other forms of diabetes in europe in early 2023. *Life 2023, Vol. 13, Page 783*, 13, 783.

Boughton, C.K., Hartnell, S., Allen, J.M., and Hovorka, R. (2019). The importance of prandial insulin bolus timing with hybrid closed-loop systems. *Diabetic Medicine*, 36, 1716–1717.

Cai, D., Liu, W., Dassau, E., Iii, F.J.D., Cai, X., Wang, J., Ji, L., and Shi, D. (2020). An adaptive disturbance rejection controller for artificial pancreas. *IFAC-PapersOnLine*, 53, 16372–16379.

Colmegna, P., Pena, R.S.S., Gondhalekar, R., Dassau, E., and Doyle, F.J. (2014). Reducing risks in type 1 diabetes using $\{\langle\}_\infty$ control. *IEEE Transactions on Biomedical Engineering*, 61, 2939–2947.

Dalla Man, C., Micheletto, F., Lv, D., Breton, M., Kovatchev, B., and Cobelli, C. (2014). The uva/padova type 1 diabetes simulator. *Journal of Diabetes Science and Technology*, 8, 26–34.

Dovc, K., Piona, C., Mutlu, G.Y., Bratina, N., Bizjan, B.J., Lepej, D., Nimri, R., Atlas, E., Muller, I., Kordonouri, O., Biester, T., Danne, T., Phillip, M., and Battelino, T. (2020). Faster compared with standard insulin aspart during day-and-night fully closed-loop insulin therapy in type 1 diabetes: A double-blind randomized crossover trial. *Diabetes Care*, 43, 29–36.

Faradji, R.N., Uribe-Wiechers, A.C., and de la Maza Viadero, M.E.S. (2019). *Hypoglycemia: Diagnosis, Management, and Prevention*, 629–653. Springer International Publishing.

Gingras, V., Taleb, N., Roy-Fleming, A., Legault, L., and Rabasa-Lhoret, R. (2018). The challenges of achieving postprandial glucose control using closed-loop systems in patients with type 1 diabetes. *Diabetes, Obesity and Metabolism*, 20, 245–256.

Gondhalekar, R., Dassau, E., and Doyle, F.J. (2016). Periodic zone-mpc with asymmetric costs for outpatient-ready safety of an artificial pancreas to treat type 1 diabetes. *Automatica*, 71, 237–246.

Goodwin, G.C., Medioli, A.M., Carrasco, D.S., King, B.R., and Fu, Y. (2015). A fundamental control limitation for linear positive systems with application to type 1 diabetes treatment. *Automatica*, 55, 73–77.

Haidar, A., Tsoukas, M.A., Bernier-Twardy, S., Yale, J.F., Rutkowski, J., Bossy, A., Pytka, E., Fathi, A.E., Strauss, N., and Legault, L. (2020). A novel dual-hormone insulin-and-pramlintide artificial pancreas for type 1 diabetes: A randomized controlled crossover trial. *Diabetes care*, 43, 597–606.

Heusden, K.V., Dassau, E., Zisser, H.C., Seborg, D.E., and Doyle, F.J. (2012). Control-relevant models for glucose control using a priori patient characteristics. *IEEE Transactions on Biomedical Engineering*, 59, 1839–1849.

Homayounzade, M. (2022). Positive input observer-based controller design for blood glucose regulation for type 1 diabetic patients: A backstepping approach. *IET Systems Biology*, 16, 157–172.

Lin, S.K. and Fang, C.J. (1997). Nonovershooting and monotone nondecreasing step responses of a third-order siso linear system. *IEEE Transactions on Automatic Control*, 42(9), 1299–1303.

Nwokolo, M. and Hovorka, R. (2023). The artificial pancreas and type 1 diabetes. *The Journal of Clinical Endocrinology & Metabolism*.

Sala-Mira, I., Garcia, P., Díez, J.L., and Bondia, J. (2022). Internal model control based module for the elimination of meal and exercise announcements in hybrid artificial pancreas systems. *Computer Methods and Programs in Biomedicine*, 226, 107061.

Sanz, R., García, P., Romero-Vivó, S., Díez, J., and Bondia, J. (2023). Near-optimal feedback control for postprandial glucose regulation in type 1 diabetes. *ISA transactions*, 133, 345–352.

Sanz, R., Garcia, P., Diez, J.L.L., and Bondia, J. (2021). Artificial pancreas system with unannounced meals based on a disturbance observer and feedforward compensation. *IEEE Transactions on Control Systems Technology*, 29, 454–460.

Sereno, J.E., Caicedo, M.A., and Rivadeneira, P.S. (2018). Artificial pancreas: glycemic control strategies for avoiding hypoglycemia. *Dyna*, 85(207), 198–207.